IOP Conference Series: Earth and Environmental Science

PAPER • **OPEN ACCESS**

Research on the characteristics of real-world vehicle particle number and mass emissions

To cite this article: Zhiwen Yang *et al* 2021 *IOP Conf. Ser.: Earth Environ. Sci.* **831** 012013

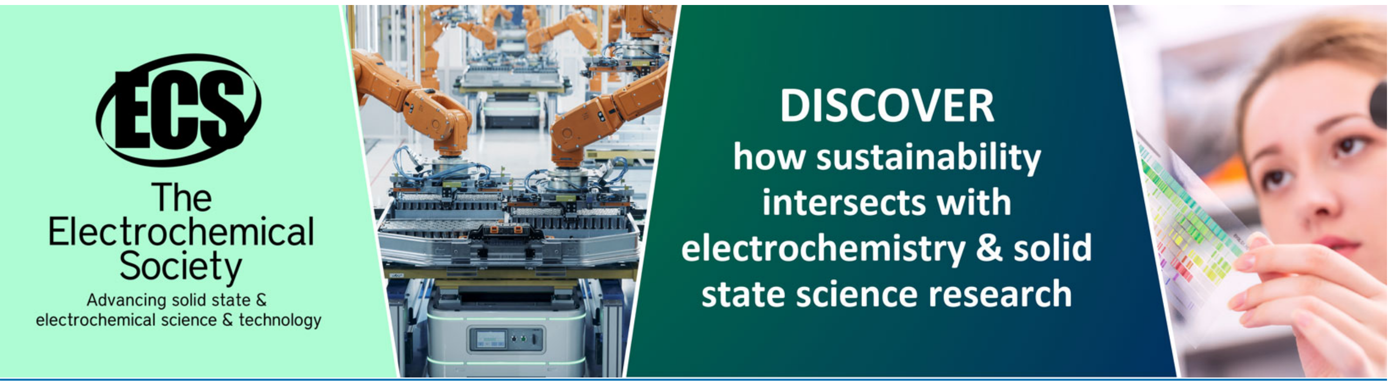

Research on the characteristics of real-world vehicle particle number and mass emissions

Zhiwen Yang[1,*], Xiaowen Zhang[1], Zhenkai Xie[1], Songbo Qi[1], Jiguang Wang[1], Jingyuan Li[1], and Mengliang Li[1]

[1]China Automotive Technology & Research Center Co., Ltd, Tianjin, 300300, China

*Corresponding author: yangzhiwen@catarc.ac.cn

Abstract. Plug-in hybrid electric vehicles (PHEVs) have been greatly promoted due to their advantages in both performance and energy saving. However, real-world particle emission measurements for PHEV are generally conducted by dilution system but rarely through the directly hot-sampling method. This study firstly employs a hot-sampling HT-ELPI+, the main component of a portable emission measurement system, to investigate the real-world emissions of particle matter (PM) and particle number (PN) from a Euro V PHEV. Obvious higher emission factors (EFs) of PN and PM occurred on the highway compared to those on other road types. However, the lowest EFs occurred on the urban road for PN, while on the rural road for PM. The average speed-bin EFs of PN and PM both exhibited increasing trends with the speed increase, especially when the speed exceeds 100 km/h. And the peak PN and PM emission rates in different speed ranges exhibit the highest in the high-speed range, while the lowest in the low-speed range. Furthermore, the particle number size distribution exhibited an obvious unimodal distribution (mode size: 9 nm) for the whole speed and the medium- and high-speed ranges, while a bimodal distribution (mode size: 9 nm and 30 nm) for the low-speed range.

1. Introduction

With the rapid increase in vehicle population and activity, the vehicle has grown to be an increasing source of gaseous and particle pollutants that influencing air quality in urban areas[1, 2]. Compared to the strength in reducing vehicle gaseous and particle mass (PM) emissions, the control requirements in particle number (PN) emissions, are relatively loose. The PN emissions from light-duty vehicles in China are not limited until the implication of national stage 6 that setting the not-to-exceed (NTE) limit of 6×10^{11} #/km for laboratory test over the WLTC and the NTE limit of 1.26×10^{12} #/km for the real driving emission test. Therefore, conducting PN emission measurements on vehicles, especially those complying with the national stage below 6, will be beneficial to evaluate the PN emission level of vehicles and formulate vehicle particle emission control management policies.

As to the vehicle exhaust particle emission characteristics, a large number of relevant studies have been done at home and abroad. Compared to conventional engine vehicles, hybrid electrical vehicles (HEVs) generally generated much higher real-world PN emissions due to that the PN emissions are more easily produced at engine start[3]. Especially due to the enriched air-fuel mixtures and lowered catalyst conversion efficiencies caused by the higher frequency of engine stop-and-goes for hybrid vehicles, HEVs frequently fail to reach the existing RDE limits[4]. With the rapid increase in HEVs population, the investigations on real-world exhaust PN emission will be increasingly vital for the HEVs particle emission control.

However, most studies against vehicle exhaust PN emissions are focused on particles with a diameter above 23 nm due to the absence of limitations on particles with a diameter below 23 nm in the requirements of China 6. Furthermore, the exhaust PN emissions of most studies are obtained by dilution system, which may exist a risk of particle conversion caused by the condensation and thus bias the particle results. To investigate the real-world particle emissions, a Euro V plug-in hybrid electric vehicle (PHEV) was tested using a portable emission measurement system (PEMS) under real-world driving conditions. And the particle with a diameter between 0.006 and 2.5 μm was directly hot-sampled without a dilution system. PN and PM emission measurements on the PHEV under uncharged initial battery state of charge were elaborately considered, to reduce the negative effect of engine stop-and-goes for hybrid vehicles. Besides, to fully analyze the emission characteristics under different driving conditions, the road type-based PN and PM emission factors (EFs), speed-bin EFs, and operating mode vehicle specific power (VSP)-bin emission rates were evaluated. Furthermore, the particle number size distributions (PSDs) under different driving modes and speed intervals were also analyzed.

2. Materials and Methods

2.1. Test Vehicles and Routes

Real-world emission measurements on a Euro V PHEV were conducted in February 2019 in Tianjin city, China. During test periods, the ambient temperature and relative humidity were averaged as 6.0±2.5 ℃ and 65.0±8.6 %, respectively. Detailed information about the tested PHEV is demonstrated in Table 1. The E10 ethanol-blended gasoline used here was acquired directly from the local market. A typical route with a length of 74 km was chosen to conduct the PEMS test, which is mainly covered by urban, rural, and highway. To investigate the characteristics of real-world driving emissions emitted by the tested PHEV under various traffic situations in Tianjin as much as possible, a total of 3 trip tests were carried out during the test. To avoid the differences in test results caused by the inconsistent driving habits of different drivers, one driver was arranged to drive the tested vehicle successively.

Table 1. Test vehicle specifications

Parameters	PHEV
Vehicle model	GEELY Borui GE
Fuel type	E10
Gross/Curb weight (t)	1.79/2.16
Engine type	Turbocharged + direct injection +DOHC
Max. combustion engine power (kW/Nm)	192/425
Max. electric engine power (kW/Nm)	60/160
Displacement (L)	1.5
After-treatment	TWC
Emission standard	Euro V
Model year	2018.11
Odometer (km)	4680
Gear	Automatic 7

2.2. Measurement system

In this study, the real-world instantaneous and cumulative emissions of gaseous and particles were collected by a united PEMS consisting of a SEMTECH-DS and an ELPI+. Besides, several other units fixed around the vehicle body were also included, such as a SEMTECH High-Speed Exhaust Flow Meter (SEMTECH EFM-HS) to continuous and direct monitor the vehicle exhaust flow, a temperature probe to monitor the exhaust temperature near the exit of the tailpipe, a GPS to acquire vehicle speed and location information (i.e., altitude, latitude, and longitude), and a weather probe for the ambient temperature and relative humidity. The gaseous were not analyzed herein. The ELPI+, developed by Dekati Ltd., was utilized to classify particles over an aerodynamic diameter range of 6 nm~10 μm in a flow rate of 10 L/min. Particles in this study were directly measured by the ELPI+ without a dilution system but equipped with a specialized external heating device[5]. By heating the impactor, the heating device allows direct measurement of up to 180℃ aerosol samples from the exhaust pipe. Additionally, the heating device and the sampling tube near the exit of the exhaust flow meter of the PEMS were connected by a 1.5 m heated sampling line, the temperature of which was controlled and maintained stability around 180℃ by a secondary integrated digital control unit.

The lithium battery was employed to power the PEMS instrument to make sure that the vehicle engine operation will not be affected by the power demand of the device. All data acquired in this study were recorded at a frequency of 1 Hertz. The whole PEMS together with the co-driver, with a total weight being around 120 kg, resulted in 5.6% of the curb weight of the tested vehicle. Meanwhile, purging and zero flow verifying were also conducted for the EFM and ELPI+ before and after each test. Besides, a laptop computer, connected to the instrument by the local area network, was employed to monitor the real-time operational status of the device.

2.3. Vehicle Specific Power

Vehicle Specific Power (VSP), defined as the instantaneous engine power output per vehicle unit mass (kW/ton), is also used herein to further reflect the gaseous emission characteristics and the differences in emissions between different initial power states under various operating modes. According to the MOVES[6], based on instantaneous vehicle speed, acceleration, vehicle mass, and road load coefficients, VSP can be calculated as the following equation:

$$\mathrm{VSP} = \frac{A}{M} \cdot v + \frac{B}{M} \cdot v^2 + \frac{C}{M} \cdot v^3 + a \cdot v + \mathrm{g} \cdot v \cdot sin\theta \tag{1}$$

Where M is the gross mass of individual test vehicle (tons), v is the vehicle speed (m/s), a is the vehicle acceleration (m/s^2), g is the gravitational acceleration (9.81 m/s^2), and θ is the road grade (radians). The road load coefficients of A (kW s/m), B (kW s^2/m^2), and C (kW s^3/m^3) represent the coefficients of the rolling resistance, rotational resistance, and aerodynamic drag, respectively. Obtained from the MOVES model, the values of A, B, and C coefficients are 0.13810, 0.00177, and 0.00043 for the light-duty tested vehicle herein. The road grade can be regarded as 0 due to the relatively flat area for the test route with elevation gain less than 15 m over 20 km[7].

3. Results & Discussion

3.1. Effects of road types on exhaust emissions

To investigate the effect of various road types with different driving conditions on the PN and PM emissions emitted by the tested vehicle, the road types herein are mainly classified based on the speed referring to the Real Driving Emissions (RDE) legislation[8]. The on-road PN and PM EFs of the vehicle tested on different road types are demonstrated in Fig.1. Besides, the driving parameters of the tested vehicle under different road types are demonstrated in Table 2. It is clear that with the average speed increase from urban, rural to the highway, the cruise fraction also exhibits an increasing trend, while the relative positive acceleration (RPA)[9], acceleration fraction, and deceleration fraction present decreasing trends. Consequently, compared to the complex traffic conditions on the urban road, the traffic behaviors on the rural road, especially on the highway, are relatively more stable due to the lower frequency and strength of acceleration and deceleration.

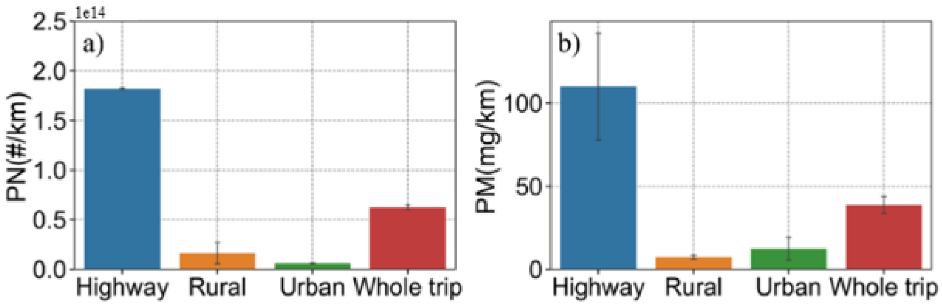

Fig. 1. Average EFs of (a) PN and (b) PM on different road types

As shown in Figure 1, the EFs on the highway, rural and urban road are $(1.8\pm0.0)\times10^{14}$, $(1.6\pm1.4)\times10^{13}$, $(6.2\pm0.3)\times10^{12}$, and $(6.3\pm0.3)\times10^{13}$ #/km, respectively, for the PN; and being 110±46, 7±2, 12±10, and 39±7 g/km, respectively, for the PM. Obvious higher EFs of PN and PM occurred on the highway compared to those on other road types, which is probably related to the markedly larger average speed and cruise fraction as shown in Table 2. However, the lowest EFs occurred on the urban road for PN, while on the rural road for PM. Compared to PN, the PM is more easily produced under the driving conditions with lower speed and higher frequency and strength of acceleration (Table 3). Consequently, the PM and PN are both easily produced under severe engine working conditions with extraordinary high speed, but the PM tends to be more easily generated under poor driving conditions with low speed and high frequency and strength of acceleration when compared to PN.

.Table 2. The real-world driving parameters of the tested vehicle

Parameters	Urban	Rural	Highway	Whole trip
Trip distance（km）	24.1±1.8	29±2.6	21.3±2.5	74.4±0.1
Avg. speed (km/h)	27.1±3.5	74.7±0.9	107.0±1.6	50.2±5.0
Acceleration fraction (%)	28.7±1.8	24.3±1.9	14.5±1.8	25.5±0.7
Cruise fraction (%)	20.7±1.8	53.3±4.8	74.5±3.0	36.5±2.9
Deceleration fraction (%)	30.2±2.5	22.4±2.9	11.0±1.5	25.5±1.2
Idle fraction (%)	20.4±5.6	0	0	12.5±3.9

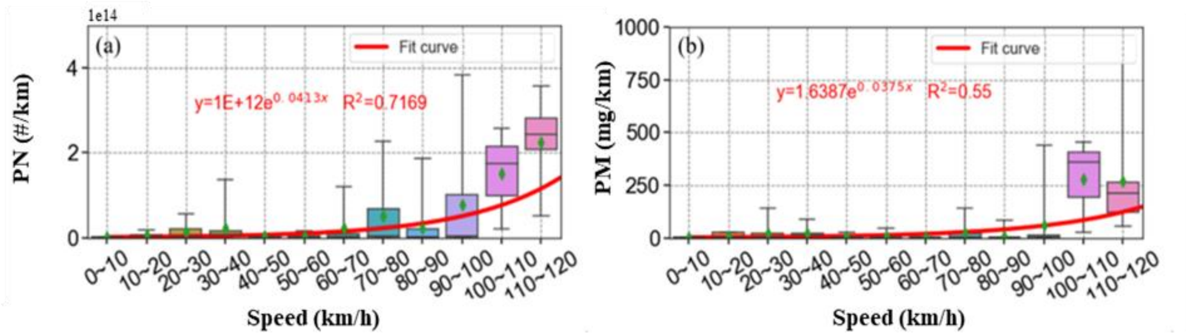

Fig. 2. Average speed-bin and the boxplot of EFs of (a) PN and (b) PM

3.2. Effects of driving modes on exhaust emissions

To investigate the variation of PN and PM EFs under different speed bins for the tested vehicle, the calculation method of EFs for each speed range in the COPERT model was drawn in this study[10]. The average speed-bin PN and PM EFs herein are obtained firstly by integrating exhaust particle emissions from on-road tests over micro-trips with 1 km distance to obtain the EFs for these trips[11], and then by averaging the EFs over different speed ranges of 10 km/h split by the average micro-trip speeds.[6] The relationships between average speed and average speed-bin PN and PM EFs (yellow diamonds) for the tested vehicle are illustrated in Fig. 2. The average speed-bin EFs of PN and PM both exhibit obvious exponential function relationships with vehicle speed, with the correlation coefficient (R2) at 0.55-0.7169. Besides, the average speed-bin EFs of PN and PM both exhibit increasing trends with the speed increase, especially when the speed exceeds 100 km/h, which is consistent with the result in Section 3.1.

To further clarify the effect of driving conditions on particle emissions, the relationship between VSP and particle emission rates is analyzed and demonstrated in Fig. 3. The PN and PM emission rates generally increase with VSP in the low-, medium-, and high-speed ranges, which is following the result in the previous study[12]. The peak PN and PM emission rates in different speed ranges exhibit the highest in the high-speed range, while the lowest in the low-speed range. Meanwhile, the peak emission rates for PN in the low-, medium-, and high-speed ranges are $1.8×10^{11}$, $1.6×10^{12}$, and $8.6×10^{12}$ #/s, respectively; and those for PM are 2.7, 4.8, and 10.7 mg/s, respectively. Besides, obvious higher VSP-bin PN and PM emission rates occur in the high-speed range relate to those in the low- and medium-speed ranges. This is in accordance with the fact that the peak emission rates for PN and PM occur in speed and acceleration bins with speeds above 95 km/h. Consequently, the particle emission control should be mainly focused on the severe engine working conditions caused by the high speed.

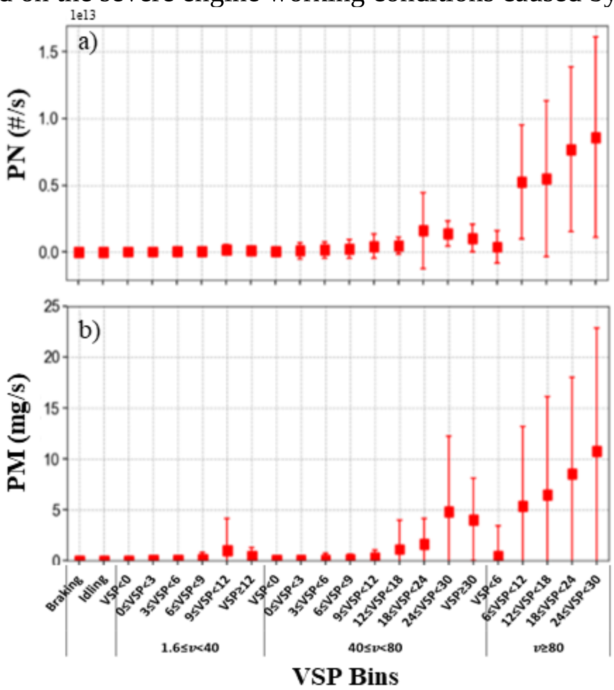

Fig. 3. Variations of average VSP-bin gaseous emission rates of (a) PN and (b) PM

3.3. Effects of operating mode on particle number size distribution

The PSDs for the tested vehicle under different driving speeds and modes were demonstrated in Fig. 4. The PSD exhibits an obvious unimodal distribution (mode size: 9 nm) for the whole speed and the medium- (60<V<90 km/h) and high-speed (V>90 km/h) ranges, while a bimodal distribution (mode size: 9 nm and 30 nm) for the low-speed range (V<60 km/h). This fact indicates that the particles with the size of around 9 nm are more easily generated with the speed increase. The peak mode size of the low-speed range here is consistent with the result on the urban road in a previous study[13]. In addition, the peak PN concentration of the acceleration mode is larger than that of other driving modes when the speed is below 90 km/h. However, when the speed is above 90 km/h, the peak PN concentration of the cruise mode is larger than that of other driving modes. The PN emissions emitted during the driving conditions with a speed below 90 km/h are mainly generated by the engine load caused by the acceleration movements, while the PN emissions emitted under the high driving speed conditions are mostly produced due to the full combustion that happened during the cruise mode.

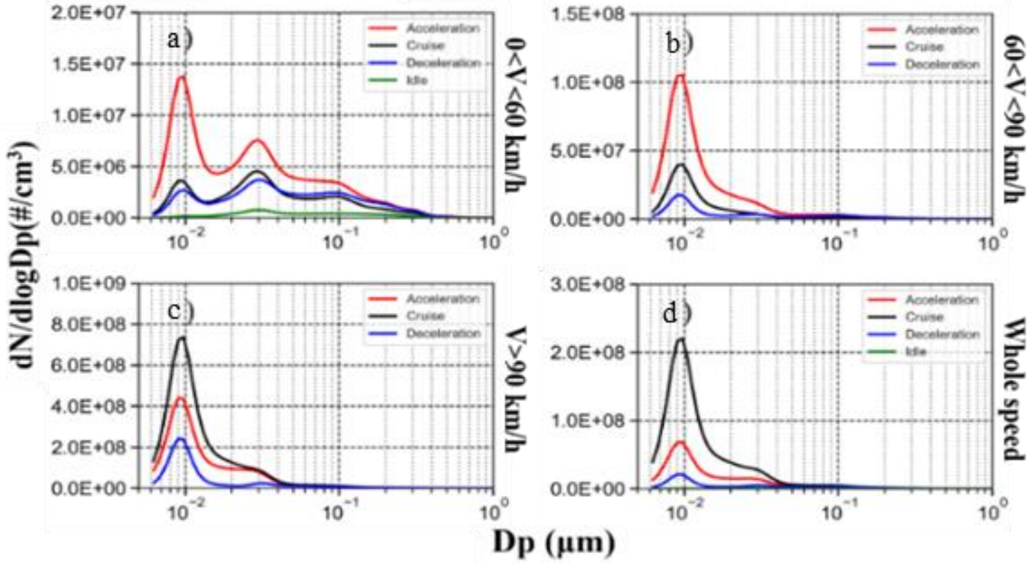

Fig. 4. Variations of the PN size distribution under different speed and driving conditions

4. Conclusions

1) The EFs on the highway, rural road, urban road, and whole trip are $(1.8\pm0.0)\times10^{14}$, $(1.6\pm1.4)\times10^{13}$, $(6.2\pm0.3)\times10^{12}$, and $(6.3\pm0.3)\times10^{13}$ #/km, respectively, for the PN; and being 110±46, 7±2, 12±10, and 39±7 mg/km, respectively, for the PM. Obvious higher EFs of PN and PM occurred on the highway compared to those on other road types. However, the lowest EFs occurred on the urban road for PN, while on the rural road for PM.

2) Obvious exponential function relationships were found between the average speed-bin EFs of PN and PM and vehicle speed. The average speed-bin EFs of PN and PM both exhibited increasing trends with the speed increase, especially when the speed exceeds 100 km/h. Besides, the PN and PM emission rates generally increase with VSP in the low-, medium-, and high-speed ranges. And the peak PN and PM emission rates in different speed ranges exhibit the highest in the high-speed range, while the lowest in the low-speed range.

3) The PSD exhibited an obvious unimodal distribution (mode size: 9 nm) for the whole speed and the medium- (60<V<90 km/h) and high-speed (V>90 km/h) ranges, while a bimodal distribution (mode size: 9 nm and 30 nm) for the low-speed range (V<60 km/h). In addition, the peak PN concentration of the acceleration mode is obviously larger than that of other driving modes when the speed is below 90 km/h. However, when the speed is above 90 km/h, the peak PN concentration of the cruise mode is larger than that of other driving modes.

References

[1] Zheng, X., Wu, Y., Zhang, S., Hu, J., Zhang, K. M., Li, Z., He, L., &Hao, J. (2017). Characterizing particulate polycyclic aromatic hydrocarbon emissions from diesel vehicles using a portable emissions measurement system. Scientific Reports, 7 (1), 10058.

[2] Winkler, S. L., Anderson, J. E., Garza, L., Ruona, W. C., Vogt, R., &Wallington, T. J. (2018). Vehicle criteria pollutant (PM, NOx, CO, HCs) emissions: how low should we go? npj Climate and Atmospheric Science, 1 (1), 26.

[3] Robinson, M. K. and Holmén, B. A. (2011). Onboard, Real-World Second-by-Second Particle Number Emissions from 2010 Hybrid and Comparable Conventional Vehicles. Transportation Research Record, 2233 (1), 63-71.

[4] Yang, Z. J., Ge, Y. S., Thomas, D., Wang, X., Su, S., Li, H., &He, H. W. (2019). Real driving particle number (PN) emissions from China-6 compliant PFI and GDI hybrid electrical vehicles. Atmospheric Environment, 199, 70-79.
[5] HT-ELPI+. *High Temperature ELPI®+*. https://www.dekati.com/products/high-temperature-elpi/.
[6] Yang, Z., Peng, J., Wu, L., Ma, C., Zou, C., Wei, N., Zhang, Y., Liu, Y., Andre, M., Li, D., &Mao, H. (2020). Speed-guided intelligent transportation system helps achieve low-carbon and green traffic: Evidence from real-world measurements. Journal of Cleaner Production, 268, 122230.
[7] Luján, J. M., Bermúdez, V., Dolz, V., &Monsalve-Serrano, J. (2018). An assessment of the real-world driving gaseous emissions from a Euro 6 light-duty diesel vehicle using a portable emissions measurement system (PEMS). Atmospheric Environment, 174, 112-121.
[8] EU (2017). Commission regulation (EU) 2017/1151. Off J Eur Union, 1 – 643.
[9] Yang, Z., Liu, Y., Wu, L., Martinet, S., Zhang, Y., Andre, M., &Mao, H. (2020). Real-world gaseous emission characteristics of Euro 6b light-duty gasoline- and diesel-fueled vehicles. Transportation Research Part D: Transport and Environment, 78.
[10] Samaras, C., Tsokolis, D., Toffolo, S., Garcia-Castro, A., Vock, C., Ntziachristos, L., &Samaras, Z. Limits of Applicability of COPERT Model to Short Links and Congested Conditions. in 20th International Transport and Air Pollution Conference 2014. 2014.
[11] O'Driscoll, R., ApSimon, H. M., Oxley, T., Molden, N., Stettler, M. E. J., &Thiyagarajah, A. (2016). A Portable Emissions Measurement System (PEMS) study of NOx and primary NO2 emissions from Euro 6 diesel passenger cars and comparison with COPERT emission factors. Atmospheric Environment, 145, 81-91.
[12] Zhang, S., Wu, Y., Hu, J., Huang, R., Zhou, Y., Bao, X., Fu, L., &Hao, J. (2014). Can Euro V heavy-duty diesel engines, diesel hybrid and alternative fuel technologies mitigate NOx emissions? New evidence from on-road tests of buses in China. Applied Energy, 132, 118-126.
[13] Li, T., Chen, X., &Yan, Z. (2013). Comparison of fine particles emissions of light-duty gasoline vehicles from chassis dynamometer tests and on-road measurements. Atmospheric Environment, 68, 82-91.